

Finding the Transition State of Quasi-Barrierless Reactions by a Growing String Method for Newton Trajectories: Application to the Dissociation of Methylene-cyclopropane and Cyclopropane[†]

Wolfgang Quapp,[‡] Elfi Kraka,^{*,§} and Dieter Cremer^{§,||}

Mathematical Institute, University of Leipzig, Augustus-Platz, D-04109 Leipzig, Germany, and
Departments of Chemistry and Physics, The University of the Pacific, Stockton, California 95366

Received: January 28, 2007; In Final Form: May 9, 2007

A method for finding a transition state (TS) between a reactant minimum and a quasi-flat, high dissociation plateau on the potential energy surface is described. The method is based on the search of a growing string (GS) along reaction pathways defined by different Newton trajectories (NT). Searches with the GS-NT method always make it possible to identify the TS region because monotonically increasing NTs cross at the TS or, if not monotonically increasing, possess turning points that are located in the TS region. The GS-NT method is applied to quasi-barrierless and truly barrierless chemical reactions. Examples are the dissociation of methylenecyclopropane to acetylene and vinylidene, for which a small barrier far out in the exit channel is found, and the cycloaddition of singlet methylene and ethene, which is barrierless for a broad reaction channel with C_s -symmetry reminiscent of a mountain cirque formed by a glacier.

1. Introduction

Finding a transition state (TS) on a potential energy surface (PES) is one of the most important tasks when studying reaction mechanism or reaction dynamics. The energy of a TS defines the classical barrier (activation energy) of a chemical reaction, which makes it possible to calculate reaction rate constants with the help of transition state theory. The steepest descent paths starting at the TS lead to the reactant(s) and product(s) of a reaction.

The determination of the location of a TS, and, by this, also the minimum energy paths leading to (from) it, is often difficult on multidimensional PESs, especially if the latter is rather flat in the TS region. If chemical intuition or preliminary calculations do not lead to a reliable guess of the TS location, any search for it may fail. Therefore, it is important to establish a mathematical tool that makes it possible to specify TS locations on a multidimensional PES without invoking chemically based guesses of the TS location.

The question how to locate the position of a TS is especially problematic in the case of dissociation (recombination) reactions. It is well-known that dissociation reactions of diatomic molecules are best described by a Morse curve, which asymptotically approaches the energy of the separated parts. Many dissociation reactions of polyatomic molecules behave in a similar way, i.e., the reaction leads to a degenerate TS corresponding to the dissociation plateau and the reverse reaction, the recombination reaction, proceeds without a classical barrier. However, if the recombination reaction requires some electronic structure reorganization in the separated parts upon bond formation, a small energy barrier may result, which increases with the degree of electronic reorganization. Such a

barrier is associated with a loose TS, which is difficult to locate with the help of typical TS localization procedures. Examples for these reactions are the carbene addition reactions (addition to alkenes, alkynes, or other molecules with multiple bonds) or chelotropic cycloadditions in general.

The location of a loose TS and the determination of a small energy barrier may have little chemical relevance because (a) the barrier does not lead to an activation enthalpy or (b) the resulting activation enthalpy may be too small to be measurable. Even in the first case there will be still the need to locate the TS if one wants to analyze the mechanism of such a reaction because this task requires the existence of a minimum energy path as suitable reference. The analysis can reveal the nature of the electronic structure reorganization steps, factors that make the reaction sensitive to the chemical environment (solvent, temperature, pressure, etc.), and the stereochemistry of the recombination step.

Detailed investigations of quasi-barrierless or barrierless reactions cannot be found in the literature because they critically depend on the location of the TS or any other unique point along the reaction path. Once such a point is found, one follows the downhill path into the entrance or exit channel of the reaction employing, e.g., the unified reaction valley approach (URVA)¹ for the mechanistic analysis. Without the location of a TS or any other unique point such a procedure is no longer applicable, and the mechanistic analysis is difficult to carry out.

In this work, we present a mathematical procedure, based on Newton trajectories (NTs) and the growing string method,^{2,3} that makes it possible to find a loose TS associated with a very small barrier or determine reasonable starting points for a downhill path in the true barrierless case. The paths traced out by NTs have well-defined mathematical properties; however, they do not have chemical relevance in the sense that they are not always identical to a minimum energy path leading from TS to energy minimum that is the location of either reactant or product. Only NTs without a turning point (local energy

[†] Part of the "Thom H. Dunning, Jr., Festschrift".

^{*} Corresponding author. E-mail: ekraka.at.pacific.edu.

[‡] University of Leipzig.

[§] Department of Chemistry, The University of the Pacific.

^{||} Department of Physics, The University of the Pacific.

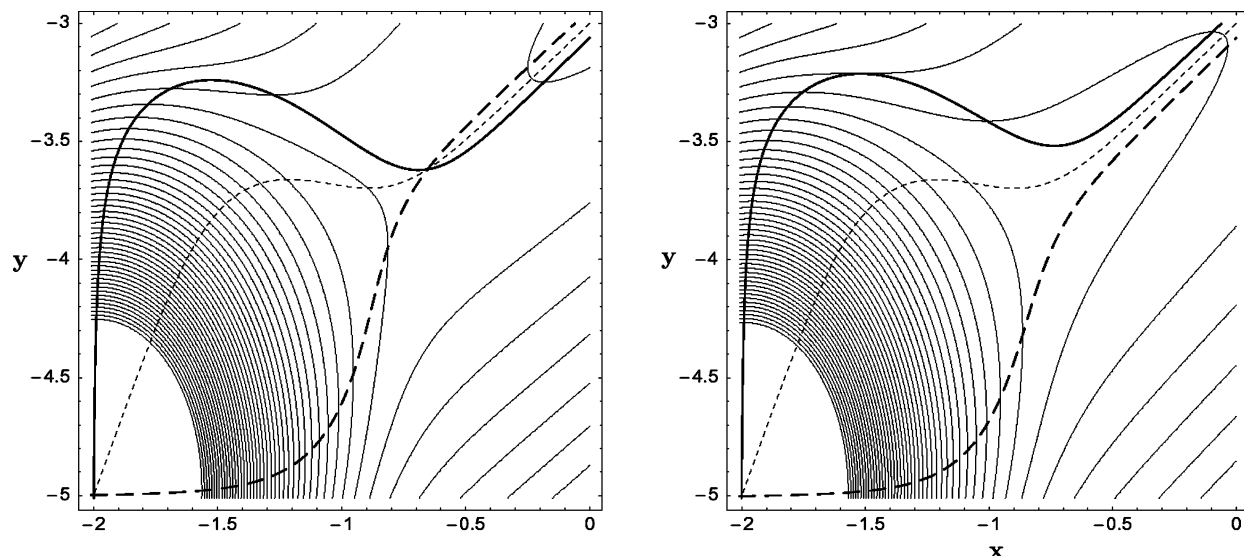


Figure 1. Two-dimensional (2D) model PES (a) with a small energy barrier (left side) and (b) without a barrier in the flat dissociation channel (right side). Three different NTs are included (bold solid, bold dashed, dashed lines), which either cross at the TS (left side) or concentrate in the dissociation channel (right side).

maximum) may serve as a minimum energy path. Use of NTs facilitates the search for TSs in extreme cases, which we will demonstrate in this work. In addition it helps to locate reasonable starting points for a downhill path that, e.g., leads directly to the product of a recombination reaction. Such a path can be used for a mechanistic analysis although it can no longer be a minimum energy path, which does not exist for barrierless reactions.

In section 2 we will shortly describe the properties of NTs and work out the procedure (a) to locate loose TSs associated with very small classical barriers and (b) to determine a reasonable starting point for a downhill path in the case of barrierless reactions. In sections 3 and 4, appropriate examples will be presented to demonstrate the usefulness of the method worked out.

2. Search for a TS Utilizing Newton Trajectories

Numerous methods have been developed with the objective of finding a first-order TS.^{2–14} Since the TS is a stationary point with a single negative Hessian eigenvalue (TS of index 1), this implies that the energy has to be maximized for one direction and minimized for all other directions. In a high-dimensional space, the direction, in which the energy has to be maximized, is difficult to determine.

Since the structures of reactant and product are known in most cases, a *one-dimensional (1D) test chain* can be developed between them. Developing all nodes (search points) of the test chain downhill narrows down the TS region and helps to find the TS between reactant and product. Various test chain methods such as the nudged elastic band method,^{2,6,7} string methods,^{3,8,9} and others⁴ have been discussed in the literature.

In conventional TS search methods, an eigenvector direction of the Hessian matrix is often assumed for uphill walking toward the TS. The eigenvector following method¹¹ used in quantum chemical programs can be applied to locate a TS, provided the latter exists in an eigenvector direction initially chosen. The method is kind of a jump method rather than the direct following of a defined curve. The next point of the search is found by maximization of the PES in the direction of the selected eigenvector as potential transition vector (under a trust region condition) and by minimization in the directions of the remainder

of the eigenvectors. In contrast, 1D search curves used in the past are NTs¹² or gradient extremals.^{13,14}

The growing string method^{3,9} used in this work follows a NT rather than searching for a steepest descent curve, i.e., an IRC (intrinsic reaction coordinate) path. For a NT, the gradient of the PES is always a pointer to a fixed direction.¹² This property can be enforced by a projection of the gradient $\mathbf{g}(\mathbf{x})$ according to eq 1.

$$\mathcal{P}_r \mathbf{g}(\mathbf{x}(t)) = \mathbf{0} \quad (1)$$

The projector \mathcal{P}_r is a constant, $n \times n$ matrix of rank $n - 1$ where n is the dimension of the PES. A unit column vector \mathbf{r} , which defines the search direction, is used for the projection. The projector, which projects orthogonal to \mathbf{r} is

$$\mathcal{P}_r = \mathbf{I} - \mathbf{r} \cdot \mathbf{r}^T \quad (2)$$

where \mathbf{I} is the unit matrix, and $\mathbf{r} \cdot \mathbf{r}^T$ is a dyadic product. Vector \mathbf{r} should be fixed for a NT adapted to any given search problem. For example, one can use as a search direction the direction to the position of the reaction product. In general however, a broad variation of different search directions \mathbf{r} is possible for NTs leading to the next stationary state of interest (see examples in Figures 1 and 2). A given value of \mathbf{r} connects the method to a fixed NT, and accordingly different \mathbf{r} values lead to a family of NTs. Every regular NT connects stationary points with an order difference of one,¹⁵ thus, for example, NTs connect minima (index 0; no negative eigenvalues of the Hessian matrix) and TSs of index 1.¹⁶

In case of a barrierless dissociation, this rule seems to fail because a NT connects a stationary point with index 0 (minimum; no negative eigenvalues of the Hessian) with a degenerate stationary point (the energy plateau) also possessing index 0. However, one has to consider that along the ascent path from minimum to energy plateau the curvature has to change from a positive to a negative value. With this change, the index of the Hessian becomes 1. Moving from the edge out onto the plateau, the index of the Hessian changes again to 0. Since only the ascent path to the edge of the energy plateau is chemically interesting, we can again utilize for the path search that NT which leads from a zero index to index 1 in the uphill direction.

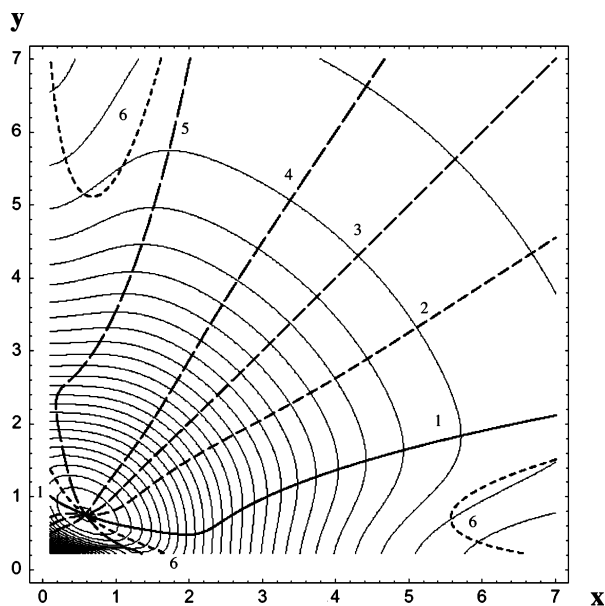


Figure 2. 2D model PES with a small, broad barrier across the flat dissociation channel. The drawn NTs are given in the following directions: (1) $f_y = 0$ (full line), (2) $0.65f_x - f_y = 0$, (3) $f_x - f_y = 0$, (4) $1.5f_x - f_y = 0$, (5) $f_x = 0$, and (6) $1.5f_x + f_y = 0$ (all dashed lines). The last NT has branches at the upper left and bottom right.

In Figure 1, it is demonstrated for 2D model potentials how NTs can be used to search for a TS in a flat dissociation channel. The special shape of the level lines in the flat region enforces the concentration of NTs starting at the minimum $(-2, -5)$ in different directions. As examples, the x -direction (bold dashed line), the y -direction (bold solid line), and the diagonal $y = x$ (dashed line) are used for three search directions of the NTs. The model surface is

$$f(x, y) = 0.6[(x - y - 3)^2 \pm 0.01(x + y - 3)^2] - 25 \exp[-3(x + 2)^2 - (y + 5)^2] \quad (3)$$

where the $+$ sign gives the left part, and the $-$ sign gives the right part of Figure 1.

Monotonically increasing NTs indicate that the PES region they pass is convex and belongs to a valley.¹⁵ The NTs turn at the point where the convex region changes to a concave or nonconvex region (the latter in the case of a plateau) and follow a path to the next stationary point. At the turning point the gradient is perpendicular to the tangent of the NT. This point is located at the border of valley and ridge.

The nature of the definition of NTs guarantees that monotonically increasing NTs, independent of their starting directions, cross at the TS (Figure 1, left) or concentrate in the exit channel (Figure 1, right). In case of a turning point (the bold solid curves in Figure 1), which corresponds to a maximal energy value along the pathway traced out by the NT and therefore should be close to a TS, this point is a useful starting point for a TS search.

Hence, a TS can be found in different ways: (1) An intersection of different NTs exists, and an estimate of the crossing point is used as the starting point for a TS optimization, which should converge within a few steps. (2) Turning points are found, which represent useful starting points for TS searches. Searches require more steps than for (1) and do not always lead to the TS in question. (3) If the NTs do not cross as shown for the second example in Figure 1 (right side), their narrowing defines the direction of the exit channel and makes it possible to find a reasonable starting point for a downhill path, which

we will demonstrate in this work (For an exception in the case of a cirque, see below.). In all cases considered, it does not make any difference whether the NT is calculated in an uphill or downhill mode, which is a clear advantage compared to steepest descent searches.

An alternate case of a dissociative channel is given in Figure 2. The minimum of the test PES is again in the left lower corner. The formula for this model surface is given by eq 4.

$$f(x, y) = 3(1 - \exp[-2(x - 0.5)])^2 \exp[-y^2] + 2(1 - \exp[-3(y - 0.7)])^2 \exp[-x^2] + 30(1 - \exp[-0.7(\sqrt{x^2 + y^2} - 1)])^2 \quad (4)$$

On the diagonal to the upper right, there is the broad border of a bowl. The ascent potential along the diagonal has the form of a Morse curve. However, the channel spreads over an area of 70° . The valley curvature uphill is stronger than its side curvature, i.e., the eigenvalue of the Hessian matrix parallel to the diagonal is significantly larger than the eigenvalue perpendicular to the diagonal. This form of a reaction valley is called a cirque¹⁷ according to its similarity with a mountain cirque carved out by a glacier. A cirque encompasses a much broader area than the streambed of a valley. Accordingly, different NTs to directions up to the bowl border spread over a wider range and do not concentrate as in the case of a reaction valley up to an energy plateau (compare Figures 1 and 2). Of the six NTs shown in Figure 2, the three central ones (NT 2, NT 3, and NT 4) are equally well suited for describing a reaction path for dissociation or recombination reaction.

Any suitable search method has to be applicable to the different situations shown in Figures 1 and 2. The Growing String-Newton Trajectory (GS-NT) method proposed in this work is based on previous developments.^{3,9,10} It uses the NT of eq 1 for any start direction (for example, \mathbf{r} can be the unit vector of the direction between the given reactant minimum and the proposed TS or the direction between the minimum and any guess point on the plateau). We search for a reaction path, which should connect the initial minimum, $\mathbf{x}_{\text{ini}} = \mathbf{x}_0$, with the end $\mathbf{x}_{\text{fin}} = \mathbf{x}_{m+1}$ by a chain of m successively calculated nodes \mathbf{x}_k .

First, a chain between the two brink points is defined by a linear combination of the corresponding structure data: we construct a number of copies of the original molecule somehow interpolated between \mathbf{x}_0 and \mathbf{x}_{m+1} .

The method alternates between predictor steps and corrector loops. If the corrector has found a node \mathbf{x}_k on the NT fulfilling an error threshold ϵ , then the next predictor will again be a linear combination (utilizing either curvilinear \mathbf{z} -matrix coordinates or Cartesian coordinates directly) of the current chain point \mathbf{x}_k and the final point. The next guess point, \mathbf{y}_{k+1} , of the string between the actual node and the final minimum is chosen by the predictor step

$$\mathbf{y}_{k+1} = \lambda_k \mathbf{x}_k + (1 - \lambda_k) \mathbf{x}_{\text{fin}}, \quad \lambda_k = \frac{m - k}{m + 1 - k} \quad k = 0, \dots, m - 1 \quad (5)$$

If the reaction path is a straight line, then the linear combination would give equidistant nodes on the line, for setting back successively $\mathbf{x}_{k+1} = \mathbf{y}_{k+1}$, without doing the corrector and then repeating ansatz (5).

After every predictor step, the GS-NT method jumps into the corrector loop. It employs a program of Gilbert and Nocedal¹⁸ in a projection version³ to find a solution of eq 1 orthogonal to the fixed search direction \mathbf{r} . It is a conjugate

gradient method, CG+, with line search, which works with Cartesian coordinates. For every reaction complex, the task emerges to determine a useful convergence condition ϵ for the norm of the projected gradient (1) of a current curve point or for every component of (1). The convergence condition ϵ should be strong enough to stop the corrector not too early before the reaction path node. However, a too strong chosen convergence condition could lead to a waste of computer time. In this situation, the corrector does ineffective calculations (*zigzagging*) while slightly sliding down along the direction of the gradient. In general, there is the possibility of a slight thinning of chain points. In the present case, we do not use any kind of elastic springs between the nodes to correct this. We simply take the result of every corrector step for a calculated chain point. In this way, the problem will nearly disappear if the search is in the flat region of the dissociative plateau of the reactions investigated in this work. There the threshold ϵ can be very small.

3. Dissociation of Methylenecyclopropene to Acetylene and Vinylidene

The cycloaddition of vinylidene in its closed shell ground state to acetylene leads in a strongly exothermic reaction (60–70 kcal/mol) to methylenecyclopropene (MCP). The cycloaddition follows the Woodward–Hoffmann rules for chelotropic reactions, i.e., the carbene adds in a nonlinear fashion to the multiple bond where the C_{2v} -symmetrical product structure is only obtained in the last step. The reaction was recently found by Cremer and co-workers to proceed with a small activation enthalpy of just 3 kcal/mol (CCSD(T)/6-311G(3df,3pd) calculations).¹⁹ DFT calculations with smaller basis sets such as 6-31G(d,p) and the B3LYP functional failed to locate a TS of index 1 for the reaction.^{19,20} Clearly, a TS should also exist in the latter case, and, therefore, it is the question how to find it.

We solved the problem by following a three-step procedure: (1) Calculate uphill paths that lead from the valley minimum occupied by MCP to the valley exit on the side of the reactants. (2) Determine points in the far valley exit that can be used as starting points for TS search procedures. (3) Calculate the location of a TS employing standard search methods.

The procedure described was applied to the chelotropic reaction between vinylidene and acetylene. For this purpose DFT calculations with the B3LYP hybrid exchange-correlation functional²¹ were carried out employing the 6-31G(d,p) basis set of Pople and co-workers.²² First, reactants and product were calculated (Figure 3). Then, we investigated for MCP three different dissociation directions into acetylene and vinylidene enforcing (a) a T-shaped (C_{2v} -symmetrical), (b) an intermediate oblique (C_s -symmetrical), and (c) a parallel C_s -symmetrical dissociation of the reactant. The geometries generated in this way were used for the fixed search direction of coarse NTs, which start at the reactant MCP. Using the GS-NT method two exit channels and two crossing points of NTs were determined on the PES, which led in subsequent TSs searches to the two TSs TS1 and TS2 shown in Figure 3.

In Figure 4, energy profiles of three calculated NTs are shown. All have pronounced turning points (here appearing as cliff points) uphill ($\epsilon = 0.03$ for the corrector threshold, step maxima = 0.5 for corrector steps, 23 nodes of the GS-NT method). Using the highest cliff point P1, a TS search²³ immediately led to TS1 (Figure 4, Table 1). A search starting at the cliff point P3 (Figure 4) resulted in the location of TS1, which is 1.2 kcal/mol below the energy of the products, however, 0.6 kcal/mol above the latter as soon as BSSE corrections²⁴ are included.

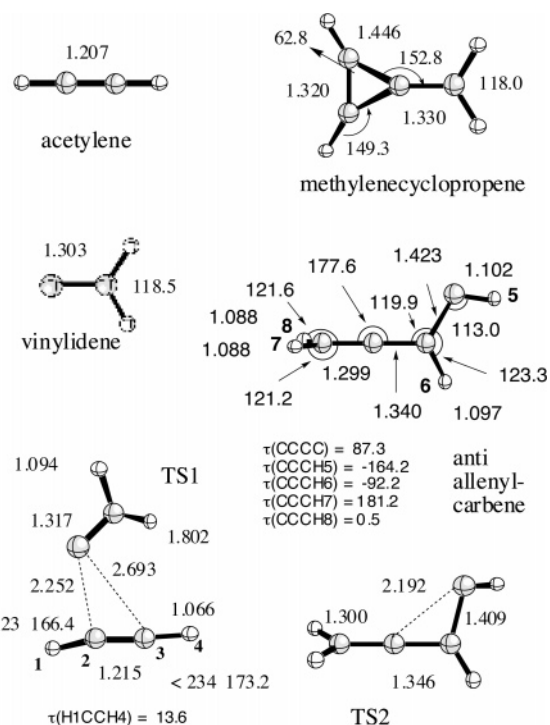


Figure 3. B3LYP/6-31G(d,p) geometries of acetylene, vinylidene, methylenecyclopropene (MCP), anti-allenylcarbene, TS1, and TS2. Distances in Å, angles in degrees.

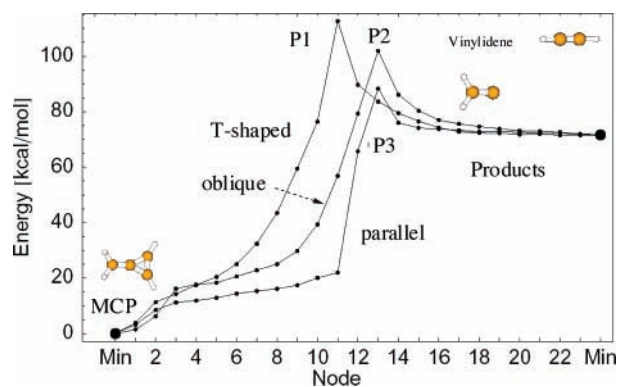


Figure 4. Energy profile of three coarse uphill NTs calculated with the GS-NT method for MCP dissociation. All NTs lead to the dissociation products vinylidene and acetylene via pronounced turning points appearing as cliff points. The three cliff points P1, P2, and P3 are reasonable starting points for TS searches.

All structures calculated on the PES were characterized by their vibrational frequencies and identifying value and mode of the one imaginary frequency in the case of a TS of index one. The relative energy of the TSs found in this work were referenced with regard to the energy of the reactants where the energy of the latter was corrected for basis set superposition errors (BSSEs) using the counterpoise method (see Table 1).²⁴ The chemical relevance of the calculated barrier values was tested by determining vibrational and thermal corrections needed to obtain activation enthalpies. TS1 was identified as a saddle point of index one according to an imaginary frequency of 182i that suggests weak interactions between the dissociating molecules vinylidene and acetylene. The calculated geometry of TS1 (Figure 3) reveals a sideward oblique position of vinylidene with C,C contact distances of 2.25 and 2.69 Å. Considering that typical C,C interaction distances for CC bond forming/braking TSs are between 1.8 and 2 Å, TS1 is certainly a loose TS, which is also in line with the fact that the geometries of

TABLE 1: Energetics of the Reaction between Acetylene and Vinylidene in Their Ground States^a

structure	sym	$E/\Delta E$	$\Delta E(\text{BSSE})$	$\Delta H(298)$	ν_{min}
acetylene ($^1\Sigma_g^+$)	$D_{\infty h}$	-77.32957			653
vinylidene ($^1\tilde{A}_1$)	C_{2v}	-77.26334			344
HCCH + H ₂ CC:		-154.59291	0	0	
MCP (1A_1)	C_{2v}	-72.4	-72.4	-67.8	361
TS1 ($^1A'$)	C_s	-1.2	0.6	-0.05	182i
TS2 ($^1A'$)	C_s	-25.6	-25.6	-23.0	216i
<i>anti</i> -allenylcarbene (1A)	C_1	-28.5	-28.5	-25.9	158

^aAbsolute energies E in hartree, relative energies ΔE in kcal/mol. $\Delta E(\text{BSSE})$ is the relative energy after counterpoise corrections for the basis set superposition error (BSSE). ν_{min} in cm^{-1} denotes the smallest vibrational frequency calculated.

acetylene and vinylidene are hardly distorted (Figure 3). The calculated geometry of TS1 reflects the fact that a carbene addition has to occur in a nonlinear (in this case C_s —rather than C_{2v} —symmetrical) mode. When investigating the chemical relevance of TS1, it was found that vibrational and thermal corrections lead to an enthalpy of 0.05 kcal/mol (Table 1) below that of the reactants. Hence, results confirm the experimental observation that the reaction proceeds without an activation enthalpy.¹⁹ Nevertheless, we can use TS1 as a meaningful starting point to carry out a mechanistic analysis of the reaction, which will be described in a forthcoming paper.

TS2 is associated with the rearrangement of MCP to allenylcarbene, which requires a cleavage of one of the three-membered ring CC single bonds. The imaginary frequency of TS2 is 216i, which is typical of CC bond cleavage processes. The distance of the cleaving bond is 2.19 Å (Figure 3). This and the fact that TS2 is characterized by an almost linear arrangement of the CH₂–C–CH unit indicates that TS2 is positioned far out in the exit channel of the rearrangement reaction leading to allenylcarbene.^{19,25} In line with this, the energy of TS2 lies only 2.9 kcal/mol above that of the 1A excited-state of *anti*-allenylcarbene (the ground state is a triplet^{19,25}). The reaction leading from MCP to allenylcarbene is endothermic by 41.9 kcal/mol ($\Delta H_f^0(298)$ difference, Table 1).

Utilizing the GS-NT method and the three-step TS search described above, we were able to find the dissociation products of MCP related to the cycloreversion of the carbene cycloaddition reaction. Dissociation can happen in a single step (TS1) or a two-step process where in the latter case the first allenylcarbene is formed (TS2) and then allenylcarbene dissociates in an endothermic reaction ($\Delta H(298^\circ) = 61.7$ kcal/mol) without barrier.¹⁹

4. Cycloaddition of Singlet Methylene to Ethene

Skell and Garner were the first to propose a mechanism for the chelotropic 1,2 cycloaddition of singlet methylene to ethene leading to cyclopropane.^{26,27} This mechanism involved in its first phase an electrophilic attack of the vacant $p\pi$ -orbital of methylene at the π -bond of ethene, polarization of the π -bond, and formation of a CC-bond between carbene and alkene. In the second phase, the methylene unit rotates into a central position and attacks via its σ electron lone pair the second C atom of the alkene in a nucleophilic way. Ample experimental and theoretical support was provided for this reaction mechanism in the past.^{28–38} Hoffmann and co-workers²⁹ demonstrated that the reaction of methylene and ethene is symmetry-allowed when the methylene follows a C_s symmetrical nonlinear (oblique) approach path, whereas it is forbidden when the reaction

complex possesses C_{2v} symmetry corresponding to a linear movement of methylene along the C_2 axis of the complex and leading to a T-structure where the top bar is the ethene molecule.

Quantum chemical calculations^{30–38} have confirmed the early predictions based on either just electronic structure considerations or orbital (state) symmetry according to the Woodward–Hoffmann rules. There are, however, two important properties of the methylene + ethene reaction that could not be predicted on just qualitative considerations: (a) The reaction proceeds without an energy barrier in the C_s -symmetrical (symmetry-allowed) reaction mode. (b) The reaction is concerted, i.e., follows a one-step mechanism contrary to what Skell and Garner^{26,27} described as a two-step mechanism. Therefore, it is more appropriate to speak of a two-phase mechanism of the reaction thus complying with its concertedness but indicating at the same time that the formation of the two CC bonds can be highly asynchronous.

Quantum chemical calculations for substituted carbenes CX₂ and higher homologues YH₂ such as germylene and stannylene³⁶ have revealed that depending on substituent X or central atom Y the chelotropic cycloaddition can change from a two-phase to a two-step, nonconcerted reaction mechanism with an intermediate carbene–alkene complex located at a minimum. The question is whether such a change in mechanism can be anticipated from a detailed analysis utilizing URVA^{1,39–42} for the methylene–ethene reaction. Such an analysis requires a TS as starting point or, in case of a barrierless reaction, another reasonable starting point in a region where the upgoing valley disembogues into the energy plateau being the location of the separated molecules methylene and ethene.

The appearance of a small, loose TS may change with the method and basis set used as was already suggested by the results of section 3. Hence, we have to verify that for the B3LYP/6-31G(d,p) description used, the reaction proceeds without classical barrier. In the latter case, there is the need to describe the valley down from the energy plateau to cyclopropane at the energy minimum. And finally, we have to calculate a suitable starting point for whatever valley situation is found.

From the discussion in connection with Figure 1, we know how NTs behave when connecting a minimum with a TS region (case a: monotonically increasing; intersecting at the TS; case b: when not monotonically increasing, turning points close to the TS). In the barrierless case these conditions continue to hold because now a degenerate TS exists, which is the energy plateau of the separated dissociation products. The intersection of NTs at the TS is missing because the TS is not of index one. However, it is still true that any NT, which increases strongly monotonically in energy (if starting at the minimum) moves automatically in a valley uphill to the next TS (basic theorem).⁴³

In Figure 5, calculated NTs for the C_s -symmetrical cycloaddition of singlet methylene to ethene are shown in a 2D subspace spanned by the x - and the z -coordinate of the methylene atom C1 where the origin of the coordinate system is given by ethene atom C3. The starting geometry of one reaction complex ring is given as well as the cyclopropane geometry at the end point of one NT (marked by larger dots). Smaller dots along the NT correspond to intermediate C1 positions, which imply small shifts in the position of C2 (generally not shown) for a fixed position of C3. Each dot is one node point of the GS-NT method. Also shown are parts of the PES in the form of contour line diagrams in a region where the valley smoothly disembogues into the plateau (109–112 kcal/mol above cyclopropane). Changes in the energy on the energy plateau are so small that contour lines and NT paths become erratic. All calculated NTs

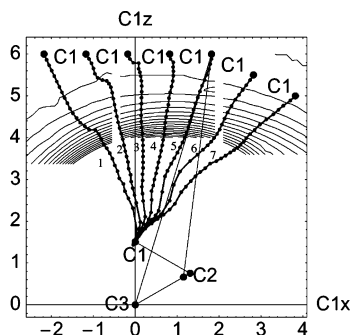


Figure 5. Seven downhill NTs (numbered 1–7) describing the cycloaddition of singlet methylene to ethene are given by the movement of atom C1 in the C_s -plane of the reaction complex. The origin of the coordinate system is atom C3 of the final structure cyclopropane. The two triangles illustrate one start and one final structure. Three parts of the PES are included between 3.5 and 6 Å. Differences of energy contour levels are 0.1 kcal/mol. They are calculated by a grid of locations for the C1-atom where C3 and the z -component of C2 are fixed. All other coordinates are minimized at every grid point. The NTs are given by connecting the calculated node points denoted by small dots.

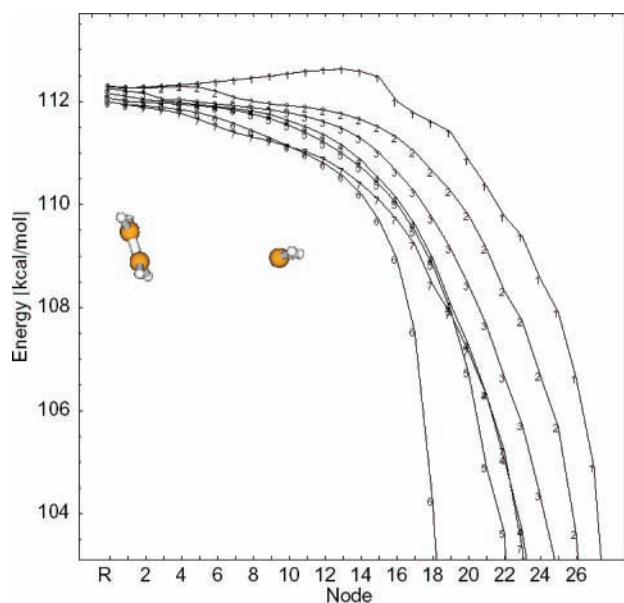


Figure 6. Energy profiles of the seven downhill NTs shown in Figure 5 calculated by the GS-NT method for the cycloaddition of singlet methylene to ethene yielding cyclopropane. Up to 33 nodes are calculated for each NT.

(up to 33 node of the GS calculated) are on the right side of the C_{2v} -symmetrical symmetry-forbidden path where the two NTs closest to this path (NT1, NT2) are effected in the way that they do no longer decrease monotonically but have to surmount first small hills in the region of the plateau (Figure 6). All other NTs possess monotonically decreasing energy profiles (Figure 6). Over a range of 50° they behave in the same way and indicate thereby the existence of a cirque rather than a valley (compare with Figure 2).

One part of the cirque in connection with the dissociation of C1 is defined on one side by the C_{2v} -symmetrical symmetry-forbidden dissociation path and on the other side by the dissociation of C1 parallel to the bond C3–C2. A bisector has been determined with regard to these extremes. The question of a starting point for a downhill URVA analysis of the reaction mechanism is solved in the way that a point, located on the bisector and lying on the edge of the energy plateau where the downhill portion of the cirque begins (at 4 Å, Figure 5), is used.

Since URVA requires second and even third derivatives of the energy, the first part of the analysis is disturbed by error progression caused by the numeric procedures used in the calculation. This part, however, is chemically not interesting with regard to both geometrical or electronic structure changes. van der Waals interactions and orbital interaction leading to bonding between the reaction partners become significant only at an approach distance of 2.5 Å and closer.

The different phases of a reaction mechanism are determined by changes in the reaction path direction, changes in the electron density distribution or the forces exerted on the atoms of the reaction complex, changes in the vibrational frequencies and the Coriolis couplings between the vibrational modes, and especially by changes in the curvature of the reaction path.^{1,39–42} Here we consider just the changes in the reaction path vector since the complete URVA analysis of the methylene–ethene cycloaddition reaction (referenced against the C_{2v} -symmetrical approach and compared for changes in substituents and central atom) is beyond the scope of the present paper and therefore a topic of another publication.

For the purpose of analyzing the direction of the reaction path given by the reaction path vector $\mathbf{t}(s)$, we decompose the latter into basis vectors $\mathbf{u}_n(s)$

$$\mathbf{u}_n(s) = \mathbf{M}^{-1} \mathbf{b}_n(s) \quad (6)$$

associated with the internal coordinates q_n used to describe the reaction complex^{1,39} (s : reaction path length; \mathbf{M} : mass matrix of the reaction complex) according to

$$\mathbf{t}(s) = \sum_{n=1}^{3K-L} t_n(s) \mathbf{u}_n(s) \quad (7)$$

where an element i of $\mathbf{b}_n(s)$ is given by $\partial q_n(\mathbf{x})/\partial x_i$, and coefficients $t_n(s)$ are determined as described by Konkoli and co-workers.³⁹ Vectors \mathbf{u}_n in eqs 6 and 7 are the internal modes that characterize the movement along the reaction path.

Amplitudes $A_{n,s}(\mathbf{t}, s)$ measure the contribution of $\mathbf{u}_n(s)$ to the reaction path direction according to

$$A_{n,s}(\mathbf{t}, s) = \frac{(\mathbf{g}^\dagger \mathbf{M}^{-1} \mathbf{b}_n)^2}{(\mathbf{g}^\dagger \mathbf{M}^{-1} \mathbf{g}) (\mathbf{b}_n^\dagger \mathbf{M}^{-1} \mathbf{b}_n)} \quad (8)$$

which considers (beside electronic effects) the kinetic aspect of the translational motion along the reaction path.

In Figure 7, the internal coordinate contributions to the reaction path vector $\mathbf{t}(s)$ are shown as a function of the reaction path parameter s . The reaction path was calculated from $s = 0$ to $s = 19 \text{ amu}^{1/2}$; however, only the range $10 < s < 19 \text{ amu}^{1/2}$ is chemically interesting because for $s < 10$ (C1,C2 distance > 2.55 Å) van der Waals interactions or even orbital interactions leading to bonding are weak. The reaction path direction depends up to $s = 16.2 \text{ amu}^{1/2}$ predominantly on the approach parameter C1C2; beyond this value vector $\mathbf{t}(s)$ depends on the C1C2C3 (CCC) bending angle or vicariously on distance C1C3. There are other small contributions to the reaction path vector throughout the reaction (see Figure 7); however, they do not play a significant role. Hence, one can distinguish two different phases in the reaction: The first one is characterized by the forming of the bond C1C2. The second one is characterized by the forming of bond C1C3 accompanied by a decrease of the bending angle C1C2C3.

On the PES, the energy decreases continuously by 112.2 kcal/mol ($\Delta H = -105.6 \text{ kcal/mol}$; exp. $\Delta H = -102 \text{ kcal/mol}$ ^{44,45})

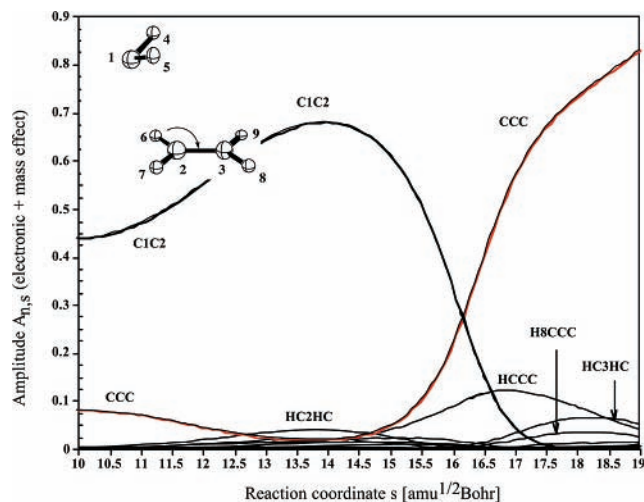


Figure 7. Characterization of the reaction path vector $\mathbf{t}(s)$ in terms of internal coordinate modes using amplitudes $A_{n,s}$, considering electronic and mass effects according to eq 8. For a definition of parameters, see insert. B3LYP/6-31G(d,p) calculations.

without giving any indication for an intermediate, i.e., the reaction is truly a concerted (one-step) barrierless reaction. However, the reaction path vector suggests a two-phase reaction mechanism with the possibility of a hidden intermediate⁴⁰ that can be transformed into a real intermediate by changing the reaction conditions (replacing H atoms against substituents X; changing C against Y; changing the environment). A two-phase reaction consisting of an electrophilic and a nucleophilic reaction phase was originally suggested by Skell and Garner²⁷ and is confirmed by our findings.

5. Conclusions

The GS method for NTs is well suited for (a) detecting a TS of a quasi-barrierless chemical reaction and (b) providing a reasonable downhill starting point for a mechanistic analysis in the case of a barrierless reaction where the TS corresponds to a high-lying energy plateau. Because the method can work in either uphill or downhill direction, it will be able to localize the interesting TS region if one starts at the minimum, which is in contrast to the steepest descent method that can proceed only downhill. In the latter case, the TS region will be missed without a good starting point.

Application of the GS-NT method to the MCP dissociation to vinylidene and acetylene led to the rapid identification of a TS representing a small barrier. In the case of the cyclopropane/ethene–methylene system a barrierless cirque was identified. A center-point in the cirque was used as starting point of the reaction analysis with the URVA method. It was shown that the reaction, although barrierless, has a two-phase mechanism, in which the electrophilic phase leading to C1C2 bond formation can be distinguished from the C1C3 bond formation of the nucleophilic reaction phase. Further investigations are in progress to clarify the chemical relevance of this observation.

Acknowledgment. This work has been supported by the National Science Foundation. E.K. and D.C. thank the University of the Pacific for supporting this work. The authors thank Dr. Hyun Joo for some preliminary calculations.

References and Notes

(1) Kraka, E. In *Encyclopedia of Computational Chemistry*; Schleyer, P. v. R., Allinger, N. L., Clark, T., Gasteiger, J., Kollman, P. A., Schaefer,

H. F., III; Schreiner, P. R., Eds.; John Wiley: Chichester, U.K., 1998; Vol. 4, p 2437.

(2) Peters, B.; Heyden, A.; Bell, A. T.; Chakraborty, A. *J. Chem. Phys.* **2004**, *120*, 7877.

(3) Quapp, W. *J. Chem. Phys.* **2005**, *122*, 174106.

(4) Maeda, S.; Ohno, K. *Chem. Phys. Lett.* **2005**, *404*, 95.

(5) Schlegel, H. B. *J. Comput. Chem.* **2003**, *24*, 1514.

(6) Henkelman, G.; Jonsson, K. *J. Chem. Phys.* **2000**, *113*, 9978.

(7) Trygubenko, S. A.; Wales, D. J. *J. Chem. Phys.* **2004**, *120*, 2082.

(8) Ren, W. E. W.; Vanden-Eijnden, E. *Phys. Rev. B* **2002**, *66*, 052301.

(9) Quapp, W. *J. Comput. Chem.* **2004**, *25*, 1277.

(10) Anglada, J. M.; Besalú, E.; Bofill, J. M.; Crehuet, R. *J. Comput. Chem.* **2001**, *22*, 387. Bofill, J. M.; Anglada, J. M. *Theor. Chem. Acc.* **2001**, *105*, 463. Crehuet, R.; Bofill, J. M.; Anglada, J. M. *Theor. Chem. Acc.* **2002**, *107*, 130.

(11) (a) Baker, J. *J. Comput. Chem.* **1992**, *13*, 240. (b) Culot, P.; Dive, G.; Nguyen, V. H.; Ghuysen, J. M. *Theor. Chim. Acta* **1992**, *82*, 189.

(12) Quapp, W.; Hirsch, M.; Imig, O.; Heidrich, D. *J. Comput. Chem.* **1998**, *19*, 1087.

(13) Hoffman, D. K.; Nord, R. S.; Ruedenberg, K. *Theor. Chim. Acta* **1986**, *69*, 265.

(14) Quapp, W.; Hirsch, M.; Heidrich, D. *Theor. Chem. Acc.* **2000**, *105*, 145.

(15) (a) Hirsch, M.; Quapp, W. *J. Mol. Struct. (THEOCHEM)* **2004**, *683*, 1. (b) Quapp, W. *J. Mol. Struct.* **2004**, *695–696*, 95.

(16) Quapp, W. *J. Comput. Chem.* **2001**, *22*, 537.

(17) Ruedenberg, K.; Sun, J.-Q. *J. Chem. Phys.* **1994**, *100*, 5836.

(18) Gilbert, J. C.; Nocedal, J. *SIAM J. Optimization* **1998**, *2*, 21.

(19) Cremer, D.; Kraka, E.; Joo, H.; Stearns, J. A.; Zwier, T. S. *Phys. Chem. Chem. Phys.* **2006**, *8*, 5304.

(20) Walch, S. P.; Taylor, P. R. *J. Chem. Phys.* **1995**, *103*, 4975.

(21) (a) Becke, A. D. *J. Chem. Phys.* **1993**, *98*, 5648. (b) Becke, A. D. *Phys. Rev. A* **1988**, *38*, 3098. (c) Lee, C.; Yang, W.; Parr, R. G. *Phys. Rev.* **1988**, *B37*, 785.

(22) Hariharan, P. C.; Pople, J. A. *Theor. Chim. Acta* **1973**, *28*, 213.

(23) Peng, C.; Ayala, P. Y.; Schlegel, H. B.; Frisch, M. J. *J. Comput. Chem.* **1996**, *17*, 49.

(24) Boys, S. F.; Bernardi, F. *Mol. Phys.* **1970**, *19*, 553.

(25) Wrobel, R.; Sander, W.; Cremer, D.; Kraka, E. *J. Phys. Chem. A* **2000**, *104*, 3819.

(26) Skell, P. S.; Garner, A. Y. *J. Am. Chem. Soc.* **1956**, *78*, 5430.

(27) Skell, P. S.; Cholod, M. S. *J. Am. Chem. Soc.* **1969**, *91*, 7131.

(28) Kirmse, W. *Carbene Chemistry*; Academic Press: New York, 1971.

(29) (a) Hoffmann, R. *J. Am. Chem. Soc.* **1968**, *90*, 1475. (b) Hoffmann, R.; Hayes, D. M.; Skell P. S. *J. Phys. Chem.* **1972**, *76*, 664.

(30) Zurawski, B.; Kutzelnigg, W. *J. Am. Chem. Soc.* **1978**, *100*, 2654.

(31) Rondan, N. G.; Houk, K. N.; Moss, R. *J. Am. Chem. Soc.* **1980**, *102*, 1770.

(32) Houk, K. N.; Rondan, N. G.; Mareda, J. *J. Am. Chem. Soc.* **1984**, *106*, 4291.

(33) Blake, J. F.; Wierschke, S. G.; Jorgensen, W. L. *J. Am. Chem. Soc.* **1989**, *111*, 1919.

(34) Houk, K. N.; Li, Y.; Evansck, J. *Angew. Chem., Int. Ed. Engl.* **1992**, *31*, 682.

(35) Bernardi, F.; Bottoni, A.; Canepa, C.; Olivucci, M.; Robb, M. A.; Tonachini, G. *J. Org. Chem.* **1997**, *62*, 2018.

(36) Sakai, S. *Int. J. Quantum Chem.* **1998**, *70*, 291.

(37) Keating, A. E.; Merrigan, S. R.; Singleton, D. A.; Houk K. N. *J. Am. Chem. Soc.* **1999**, *121*, 3933.

(38) Blavins, J. J.; Cooper, D. L.; Karadakov, P. B. *Int. J. Quantum Chem.* **2004**, *98*, 465.

(39) Konkoli, Z.; Kraka, E.; Cremer, D. *J. Phys. Chem. A* **1997**, *101*, 1742.

(40) Cremer, D.; Wu, A.; Kraka, E. *Phys. Chem. Chem. Phys.* **2000**, *3*, 674.

(41) Kraka, E.; Wu, A.; Cremer, D. *J. Phys. Chem. A* **2003**, *107*, 9008.

(42) Kraka, E.; Cremer D. *J. Phys. Org. Chem.* **2002**, *15*, 431.

(43) (a) Hirsch, M.; Quapp, W. *J. Math. Chem.* **2004**, *36*, 307. (b) Hirsch, M.; Quapp, W. *Chem. Phys. Lett.* **2004**, *395*, 150.

(44) Cox, J. D.; Pilcher, G. *Thermochemistry of Organic and Organometallic Compounds*; Academic Press: New York, 1970.

(45) Hayden, C. C.; Neumark, D. M.; Shobatake, K.; Sparks, R. K.; Lee, Y. T. *J. Chem. Phys.* **1982**, *76*, 3607.